

A NEW SRF CAVITY SHAPE WITH MINIMIZED SURFACE ELECTRIC AND MAGNETIC FIELDS FOR THE ILC*

Zenghai Li and Chris Adolphsen, SLAC, Menlo Park, CA 94025, U.S.A.

Abstract

The TESLA TDR cavity has been chosen as the baseline design for the International Linear Collider (ILC) main linacs. There are continuous SRF R&D efforts to develop alternative cavity designs that can produce higher gradient which in turn could lead to significant cost savings in machine construction and operation. It is believed that the maximum gradient achievable in a superconducting cavity is limited by the critical magnetic flux B_c of the niobium, which is approximately 180 mT. Most of the new designs were focused on minimizing the surface magnetic field (B_s) while the requirement on electric field (E_s) was relaxed. The Low Loss design was one of the optimized designs with a B_s reduction of more than 10% over the baseline design which could support a gradient as high as 50MV/m. The E_s field in this design is however about 15% higher than the baseline design. Though it is not clear what undesirable effects the high E_s field may induce at high gradient, it is advantageous in a design with both B_s and E_s surface fields minimized. In this paper, we will present an optimized cavity shape that minimizes both the B_s and E_s fields. The design of the HOM couplers for damping the wakefields will also be presented.

INTRODUCTION

The TESLA TDR cavity shape [1], was proposed as the baseline design for the International Linear Collider (ILC) [2]. The cavity shape was optimized mainly with respect to E_s/E_a , the ratio of maximum surface electric field to the accelerating gradient, and a ratio less than 2 was achieved. This low surface field ratio was considered advantageous in suppressing electron field emission at high gradients. Remarkable progresses have been made in understanding the limitations of field gradient in a superconducting cavity since the TDR was developed. It is believed that the maximum gradient achievable in a superconducting cavity is limited by the critical magnetic flux B_c of the niobium which is approximately 180 mT [3]. The later works on the ILC cavity optimization were then aimed towards a lower B_s/E_a ratio. The Low Loss (LL) [4,5,6] cavity shape was then developed as an alternative design for the ILC. The geometry of the LL cavity is optimized to have a lower B_s/E_a ratio and a higher shunt R/Q by reducing the size of the iris and increasing the cavity volume in the high magnetic field region. As a comparison to the TDR shape, the iris radius of the LL cell is 30-mm, 5-mm smaller than TDR, and the side wall of the LL cell is more upright. These modifications resulted in more than 10% lower in B_s/E_a

and 15% higher in R/Q and geometric factor G which make the cavity more efficient in acceleration and less cryogenics loss. However, the E_s/E_a of the LL design is about 15% high than the TDR cavity. If the B field limitation is the dominant factor for reaching high gradient, the new LL shape could support an ultimate gradient of over 50 MV/m because of low B_s/E_a ratio. There are concerted efforts in various labs to fabricate and test the LL shape cavities [7,8] to realize such a gradient goal. Significant progresses have been made in high gradient testing of the LL 9-cell cavities in the past years. These efforts are on going to explore the gradient reach of such a design. Although it is not clear what undesirable effects the high surface electric field may induce at high gradients, it would be advantageous to have a cavity design that has both the E_s/E_a and B_s/E_a minimized to alienate potential side effects of high surface fields. We have recently developed a Low Surface Field (LSF) cavity shape for the ILC. This shape could potentially improve the cavity performance since both the B_s and E_s fields are lower. In this paper, we present the optimization results of the LSF shape, and the HOM coupler design to damp the harmful dipole modes.

CELL SHAPE OPTIMIZATION

Choice of Iris Aperture

A small iris opening increases the shunt impedance thus reduces the stored energy in the cell for a given gradient, and in turn lowers the surface fields. It was found however that the cell-cell coupling quickly becomes undesirably small as the iris radius becomes much smaller than 30-mm as shown in Table 1. At a lower cell-cell coupling, the field imbalance becomes more sensitive to cell dimension errors as the figure of merit for the sensitivity is N^2/k_{cc} , where N is the number of cells and k_{cc} is the cell-cell coupling. In addition, a smaller iris opening will result in higher wakefields which would tighten the alignment tolerances. So the 30-mm iris radius is chosen for the LSF design.

Table 1: Monopole bandwidth versus iris opening

iris radius (mm)	Bandwidth (MHz)
25.0	9.6
27.5	13.0
30.0 (LL & LSF)	19.2
35.0 (TDR)	24.2

Cell Profile

The new shape profile is similar to the LL shape except that the disk wall is straight up without a tilt angle. The cell contour is composed of an elliptical iris (a_n , b_n) and

* Work supported by DOE contract DE-AC02-76SF00515.

an elliptical top (*at*, *bt*) connected by straight lines, as shown in Fig. 1. For a given disk thickness T ($an=T/2$), *bn* and *bt* are optimized to minimize the surface E and B fields while cell radius “*b*” is adjusted to obtain a resonant frequency of 1.3-GHz. Fig. 2 shows the results of the surface field B_s/E_a and E_s/E_a versus disk thickness. The TDR and LL cavity designs are also shown for comparison. The best surface field solution among these designs is the one that with $an=11.8$ mm, which reduces the B_s/E_a by 11% and E_s/E_a by 5% as compared with the TDR. However it was found that the dipole modes in this design are more trapped in the cell due to the thicker iris and are difficult to be damped. The next best solution is the design with $an=10.5$ mm which is chosen as the LSF shape. This design has surface fields B_s/E_a 11% lower than the TDR and E_s/E_a 15% lower than the LL. The cell profiles and the surface fields along the cell contours of the TDR, the LL, and the LSF designs are shown in Fig. 3 for comparison.

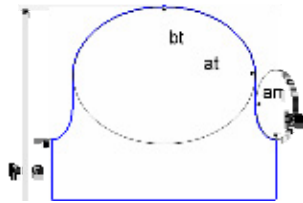


Figure 1: Cell parameters used for shape optimization.

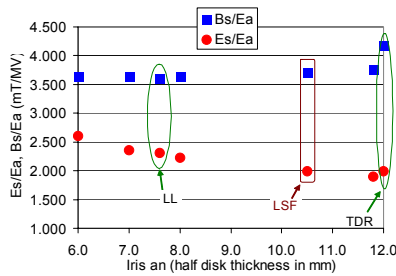


Figure 2: Surface fields vs disk thickness ($an=T/2$).

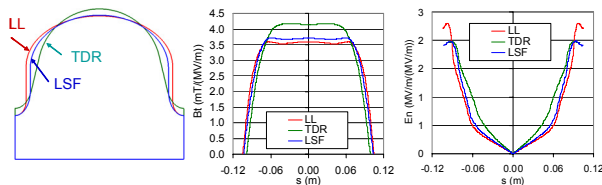


Figure 3: Cavity profile and surface field comparison between the LL (red), TDR (green), and the LSF (blue). “*s*” is the contour length of cell profile from the equator.

SENSITIVITY TO CELL ERROR

Because of the thicker disk in the new LSF design, the monopole bandwidth is about 18% narrower than the LL cavity. The field flatness in the 9-cell cavity becomes more sensitive to the cell errors as the cell-cell coupling is reduced. The field amplitude deviation in cell “*i*” due to a frequency error Δf_i in cell “*i*” can be estimated as

$$\frac{\Delta E_i}{E_i} = \frac{N^2}{k_{cc}} \cdot \frac{\Delta f_i}{f_i}$$

The cell frequency error Δf_i and the coupled mode frequency errors of the 9-cell cavity due to an geometry error in cell “*i*” has little differences between the LL and LSF designs. The field imbalance due to the cell error is then inversely proportional to the cell-cell coupling k_{cc} . Fig. 4 compares the maximum field imbalance between the three designs for a 10-micron single cell error, which corresponds to a Δf_i of 150kHz, as functions of cell number. The LSF design is about 20% more sensitive than the LL design.

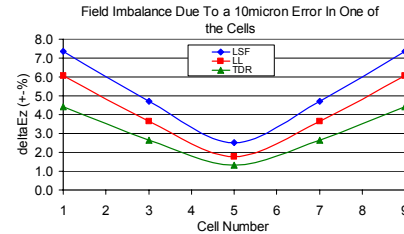


Figure 4: Field Imbalance due to a 10- μ m error in cell radius.

HOM COUPLER OPTIMIZATION

The mode spectrum and the R/Q values of the LSF design are shown in Fig. 5 up to the 3rd dipole band. The most important dipole mode is the 1pi/9 mode in the third band which has the highest R/Q. The 6pi/9 mode in the 1st band and the 5pi/9 mode in the 2nd band are also high in R/Q. The goal of the HOM coupler optimization is to damp the 3rd band high R/Q to a Qext below 10^5 , which is the ILC design requirement.

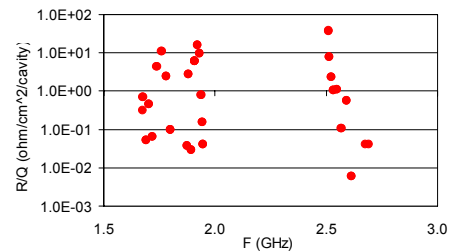


Figure 5: Dipole mode R/Q up to the third band.

End Beampipe

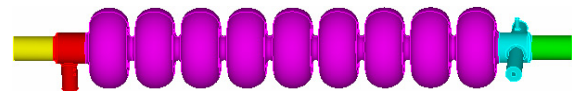


Figure 6: The 9-cell LSF cavity with coupler end-groups.

The end beampipe geometry of the LSF design is similar to the LL cavity. The beampipe radius is 38-mm in the HOM coupler region, and is tapered down to a smaller beampipe radius of 30-mm. The modes up to the 3rd band are cut off by the 30-mm beampipe ($F_c=2.9$ GHz). Thus the highest R/Q modes are damped “locally” by its own HOM couplers, not affected by adjacent cavities.

HOM Coupler

The HOM coupler has the same basic design as the TDR and LL. However, the thicker disk in the new design shifted the frequency of the 3rd band high R/Q mode about

50-MHz higher. The fields of this mode are more concentrated in the cavity than that in the LL design, as compared in Fig. 7. The HOM damper needs to be modified in order to obtain effective damping.

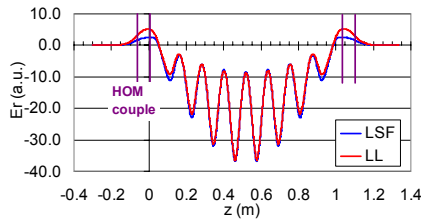


Figure 7: Field of the highest R/Q 3rd band mode.

The loop shape: The width of the loop was reduced to improve the match at the third band frequency. A nose-tip on the loop is included to enhance the electric coupling.

The loop angle: The loop angle is optimized to couple effectively to the high R/Q modes. This angle is 45 degrees with respect to the x-y plane with the hook side pointing to the cavity as shown in Fig. 8.

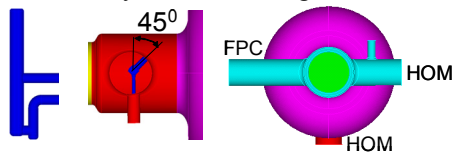


Figure 8: HOM coupler: loop shape and orientation.

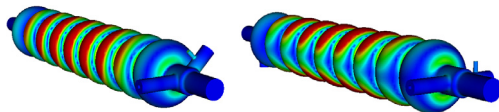


Figure 9: Mode polarization versus coupler orientations. Left) mode rotated with original LL coupler orientations; right) mode y-polarized with the new coupler orientations.

The azimuthal location of HOM couplers: The natural polarizations of the highest R/Q dipole modes in the LSF cavity are rotated about the z-axis, as shown in Fig. 9, if the HOM couplers are placed at the same azimuthal positions as in the LL design. These azimuthal positions were re-optimized for the LSF cavity such that the dominant modes, e.g. the $1\pi/9$ mode in the 3rd band, are polarized in the x or y directions. The new azimuthal positions of the HOM couplers are quite different from the LL design: the downstream HOM coupler is on the opposite side of the FPC coupler and the upstream HOM coupler is in the vertical plane as shown in Fig. 8. These new coupler orientations result in dipole modes naturally polarized in the x and y planes. An additional advantage of the new orientation is that the RF and short-range wakefield kicks due to the HOM and the FPC couplers at the downstream end partially cancel. The upstream HOM coupler has a 180 degree azimuthal rotational symmetry in terms of the coupling to the dipole modes. One can alternate this orientation among the cavities in a cryomodule to minimize the wakefield and RF kicks in the y-plane.

Damping Results

The Qext of the dipole modes were calculated using Omega3P [9] on the NERSC supercomputers. Optimized Qext for the first three dipole bands are shown in Fig 10. There are a few modes that have higher Qext, but the R/Q of these modes are low. The most important dipole mode to be damped is the $1\pi/9$ mode in the 3rd band. The Qext of this mode is below 10^5 and satisfies the ILC requirement.

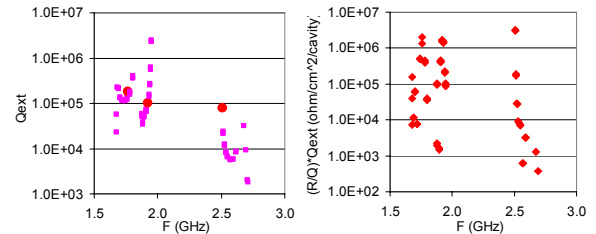


Figure 10: The damping results calculated using Omega3P: left) Qext; right) shunt impedance (R/Q)*Qext.

SUMMARY

A Low Surface Field cavity shape was optimized based on the LL cavity design. The LSF shape provides a surface magnetic field 11% lower than the TDR design and the peak electric surface field 15% lower than the original LL design. This design could potentially support 10% higher gradient than the TDR and improve the cavity performance since both the electric and magnetic surface fields are low. The HOM coupler was re-optimized for the new LSF design to damp the dipole wakefields. The Qext of the highest R/Q mode in the 3rd band is below 10^5 and satisfies the ILC requirement.

The simulation results presented in this paper was obtained using Omega3P running on NERSC computers.

REFERENCES

- [1] TESLA Collaboration.
- [2] <http://www.linearcollider.org>
- [3] K. Saito, "Fundamental RF critical Field Overview," Proc. Workshop on Pushing the Limits of RF Superconductivity, ANL, Argonne, September 2004.
- [4] J. Sekutowicz et al., "Low Loss Cavity for the 12 GeV CEBAF Upgrade", JLAB, TN-02-023, 2002.
- [5] J. Sekutowicz et al., "Design of a Low Loss SRF Cavity for the ILC," Proc. PAC05, Knoxville, 2005.
- [6] Z. Li et al., "Optimization of the Low Loss SRF Cavity for the ILC," proc. Of PAC07, Albuquerque, New Mexico, June 2007.
- [7] K. Saito et al., proc. of 12th Int. Workshop on RF Superconductivity, Ithaca, NY, July 10-15, 2005.
- [8] P. Kneisel et al., proc. of 12th Int. Workshop on RF Superconductivity, Ithaca, NY, July 10-15, 2005.
- [9] L. Lee et al., "Modeling RF Cavity with External Coupling," 2005 SIAM Conference on Computational Science and Engineering, Orlando, Florida, 2005.